

Cyclohexyl “base pairs” stabilize duplexes and intensify pyrene fluorescence by shielding it from natural base pairs†

Hiromu Kashida,* Koji Sekiguchi, Naofumi Higashiyama, Tomohiro Kato and Hiroyuki Asanuma*

Received 4th August 2011, Accepted 5th October 2011

DOI: 10.1039/c1ob06325a

In this study, we investigated the stability and structure of artificial base pairs that contain cyclohexyl rings. The introduction of a single pair of isopropylcyclohexanes into the middle of DNA slightly destabilized the duplex. Interestingly, as the number of the “base pairs” increased, the duplex was remarkably stabilized. A duplex with six base pairs was even more stable than one containing six A–T pairs. Thermodynamic analysis revealed that changes in entropy and not enthalpy contributed to duplex stability, demonstrating that hydrophobic interactions between isopropyl groups facilitated the base pairing, and thus stabilized the duplex. NOESY of a duplex containing an isopropylcyclohexane–methylcyclohexane pair unambiguously demonstrated its “pairing” in the duplex because distinct NOEs between the protons of cyclohexyl moieties and imino protons of both of the neighboring natural base pairs were observed. CD spectra of duplexes tethering cyclohexyl moieties also showed a positive–negative couplet that is characteristic of the B-form DNA duplex. Taken together, these results showed that cyclohexyl moieties formed base pairs in the DNA duplex without severely disturbing the helical structure of natural DNA. Next, we introduced cyclohexyl base pairs between pyrene and nucleobases as an “insulator” that suppresses electron transfer between them. We found a massive increase in the quantum yield of pyrene due to the efficient shielding of pyrene from nucleobases. The cyclohexyl base pairs reported here have the potential to prepare highly fluorescent labeling agents by multiplying fluorophores and insulators alternately into DNA duplexes.

1. Introduction

Natural DNA forms a stable double-helical structure, both by hydrogen bonding and aromatic stacking interactions. Natural base pairs achieve high stability and orthogonality by controlling the strength of these two interactions in a very sophisticated manner. In 1995, Kool *et al.* first reported that hydrogen bonding is not a prerequisite for the stability of the DNA duplex; an artificial base pair, which has aromatic rings but no hydrogen bonding sites, can stabilize the DNA duplex.¹ Since then, a wide variety of artificial base pairs that use aromatic stacking interactions and/or hydrogen bonding has been reported.^{2–9} In addition, non-ribose scaffolds were also utilized to design various base-surrogates involving functional molecules.^{10–17} These artificial nucleotides have the potential to serve as novel nanomaterials and biological tools.^{18–22} Furthermore, investigation into the tolerance of duplex stability by changing the structure of bases and linkers should provide insight as to why nature selected DNA as genetic carriers.

Graduate School of Engineering, Nagoya University, Furocho, Chikusa, Nagoya, 464-8603, Japan. E-mail: kashida@mol.nagoya-u.ac.jp, asanuma@mol.nagoya-u.ac.jp; Fax: +81-52-789-2528; Tel: +81-52-789-2488

† Electronic supplementary information (ESI) available: Synthetic procedures of methylcyclohexane moiety, 2D NOESY between aliphatic protons and UV-Vis spectra. See DOI: 10.1039/c1ob06325a

Recently, Leumann *et al.* incorporated a non-planar artificial base, cyclohexylbenzene, into the middle of oligodeoxyribonucleotides (ODN) *via* D-ribose.²³ Surprisingly, these base pairs greatly stabilized a DNA duplex through a cyclohexyl/phenyl interaction, suggesting that even non-planar molecules can be accommodated inside the DNA duplex. However, to our knowledge, artificial base pairs without aromatic rings have not been reported on so far, because aromatic rings have been believed to be essential to stabilize the duplex by stacking or CH– π interactions.

Previously, we reported novel “base pairs” tethering cyclohexyl moieties (**H** and **I** residues in Fig. 1b) on D-threoninol as an insulator that inhibits electron or hole transfer.²⁴ When the base pairs were introduced between nucleobases and perylene diimide (PDI), the quantum yield of PDI greatly increased. Concurrently, we found that base pairs of isopropylcyclohexane moieties (**H**) adjacent to PDI moieties stabilize the whole DNA duplex as the number of base pairs increase, even though they have neither hydrogen bonds nor aromatic stacking interactions. These results prompted us to investigate the base pairs of cyclohexyl base surrogates in detail. If non-aromatic molecules do not destabilize DNA and thus work as artificial bases, the molecules available to be incorporated into DNA should be extended, allowing for further functionalization of DNA. In this study, we first analyzed the structure and the stability of duplexes containing a cyclohexyl base pair in detail. Next, we applied the base pair as an insulator to enhance

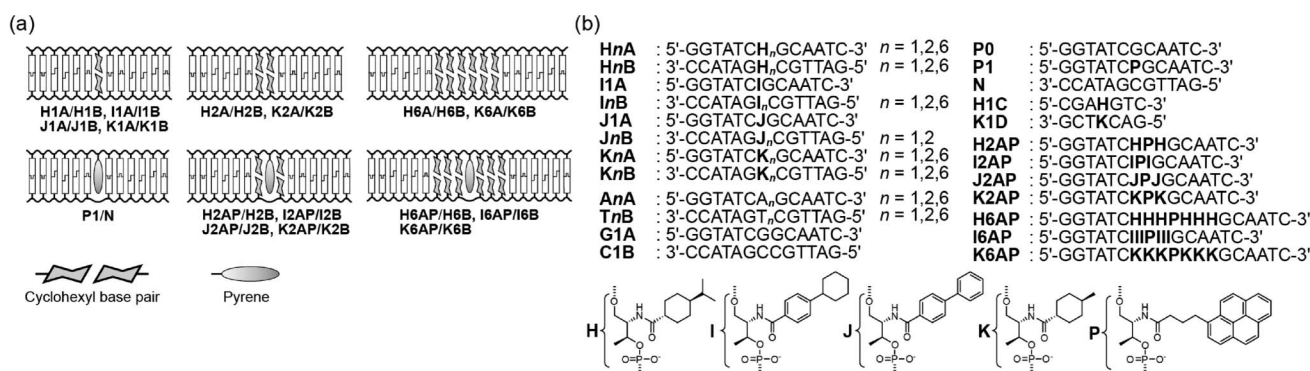


Fig. 1 (a) A schematic representation of duplexes modified with cyclohexyl base pair(s). (b) Sequences of the modified ODNs synthesized in this study. The chemical structures of insulators and fluorophore moieties are also shown.

pyrene emission, since this artificial base pair can suppress electron transfer to and from nucleobases due to the lack of π electrons.

2. Results

2.1 Structural analysis of a duplex containing artificial base pairs

We initially investigated the structure of a duplex containing a cyclohexyl base pair. If non-natural molecules work as a base pair, molecules should be located inside the DNA duplex and interact with each other. To confirm its solution structure, NMR structural analysis was conducted with a 7mer duplex (**H1C/K1D** in Fig. 1) tethering an **H-K** pair at its center position. A **K** residue was introduced into DNA *via* D-threosinol²⁵ using phosphoramidite chemistry (see Supporting Information†). In order to monitor imino protons that are exchangeable with water molecules, NMR was measured in H₂O (H₂O/D₂O, 9:1) at 275 K with a 3-9-19 WATERGATE pulse sequence for H₂O suppression.²⁶ Most of the signals of the duplex, except for the protons of the cyclohexane rings, could be assigned from the NOESY, DQFCOSY and TOCSY spectra. The one-dimensional NMR chart of the imino proton region is shown at the top of Fig. 2. Six peaks, which

correspond to six natural base pairs, were observed in the imino proton region, although the signals of imino protons of G4 and G7 overlapped. These results indicated that incorporation of a non-planar base pair did not severely disturb the base pairing of natural nucleobases. NOEs between imino protons and protons of **H** and **K** are also shown in Fig. 2. Methyl protons of **H** showed NOEs to imino protons of both of G4 and T10. Similarly, distinct NOEs were observed between methyl protons of **K** and imino protons of G4 and T10. These NOEs unambiguously demonstrated that both the isopropyl group of **H** and the methyl group of **K** were located adjacent to both G4 and T10. In addition, H_b of **H** showed NOE with an imino proton of T10, whereas H_a of **K** did so with an imino proton of G4, suggesting that the orientations of the cyclohexane rings of **H** and **K** are reversed. Intermolecular NOEs between **H** and **K** were also observed, showing that **H** and **K** are located in close proximity (see Fig. S1 in Supporting Information†). NOESY definitely demonstrated that **H** and **K** formed a “base pair” inside the DNA duplex. Computer modeling without any restraints by Insight II/Discover 3 was also consistent with the results of NOESY (Fig. 3). Thus, we concluded that cyclohexyl moieties worked as an artificial base pair; the moieties were located inside

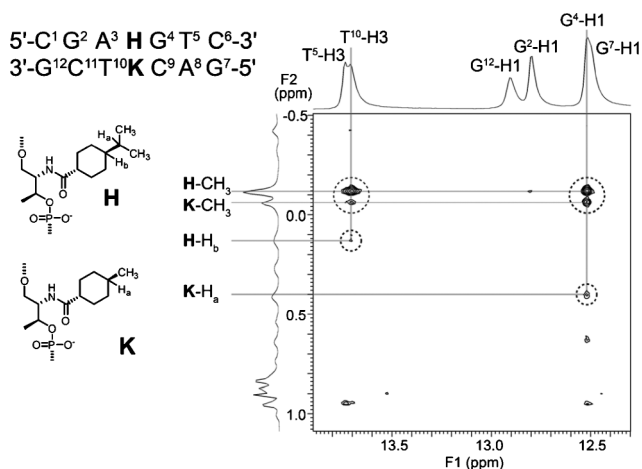


Fig. 2 2D NOESY spectra of **H1C/K1D** between the aliphatic protons and imino protons in H₂O/D₂O (9/1) at 275 K. 1D spectra of the imino protons and aliphatic protons are shown at the top and left of the chart, respectively. The residue numbers and proton numbers of **H** and **K** residues are shown at the left.

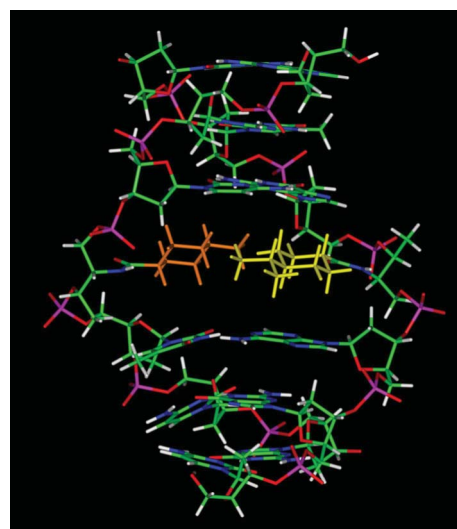


Fig. 3 Energy-minimized structure of **H1C/K1D** that contains an **H-K** pair calculated by Insight II/Discover 3. The **H** and **K** residues are colored in yellow and orange, respectively.

the duplex and interacted with each other. It should be noted that the isopropyl group of **H** and the methyl group of **K** are in close proximity, indicating that these groups interact with each other.

Next, we measured the CD spectra of duplexes containing **H–H** pairs in order to investigate the structure of a DNA duplex tethering multiple cyclohexyl base pairs, as shown in Fig. 4. **H2A/H2B** carrying two **H–H** pairs showed a similar positive couplet to that of a native duplex (**P0/N**). Similarly, the incorporation of six **H–H** pairs did not significantly alter the spectra; **H6A/H6B** showed similar spectra to those of other duplexes. These results indicated that the incorporation of **H–H** pairs did not disturb the basic B-form structure of nucleobases. From NMR and CD analyses, we concluded that cyclohexyl moieties worked as base pairs without disturbing the B-form structure, although these bases had non-planar structures.

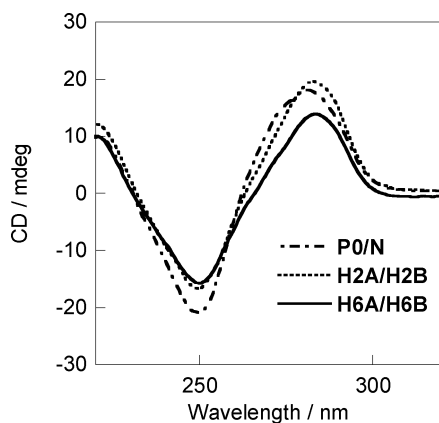





Fig. 4 CD spectra of **P0/N**, **H2A/H2B**, and **H6A/H6B** at 20 °C. Conditions: [NaCl] = 100 mM, pH 7.0 (10 mM phosphate buffer), [ODN] = 5.0 μ M.

2.2 Stability of duplexes containing artificial base pairs

We next investigated the thermal stability of duplexes containing cyclohexyl base pairs. Here, we selected four kinds of molecules as artificial bases *via* D-threosinol (**H**, **I**, **J** and **K** in Fig. 1b): **H–H** and **K–K** homo-pairs do not carry benzene rings, but have only cyclohexane rings. The **I–I** pair contains both benzene and cyclohexane rings, whereas **J–J** contains no cyclohexane rings but two benzene rings. By comparing the melting temperatures (T_m s) of duplexes involving these base pairs, the effect of aromatic rings on duplex stability was evaluated.

When a single **H–H** pair was introduced into DNA, its T_m slightly dropped compared with the native duplex; the T_m of **H1A/H1B** was 44.7 °C, whereas that of the native duplex (**P0/N**) was 47.7 °C (Table 1). The **K–K** pair that also lacks an aromatic ring (**K1A/K1B**) further lowered its T_m to 41.1 °C, indicating that cyclohexyl moieties destabilized DNA due to its non-planar structure. However, as the number of the **H–H** pairs increased, T_m did not decrease but somewhat increased. The T_m of **H2A/H2B**, which contains two **H–H** pairs, was 2.4 °C higher than that of **H1A/H1B**. Surprisingly, the incorporation of six **H–H** pairs massively stabilized the DNA duplex; the T_m of **H6A/H6B** was as high as 61.3 °C, which was 13.6 °C higher than that of **P0/N**. We also measured T_m s of native duplexes that contained A–T or G–C pairs instead of **H–H** pairs in order to compare the stabilizing

Table 1 Thermodynamic parameters of duplexes containing artificial base pairs

Sequence	$T_m / ^\circ\text{C}^a$	$-\Delta H / \text{kcal mol}^{-1}$	$-\Delta S / \text{cal}^{-1} \text{K}^{-1} \text{mol}^{-1}$	$-\Delta G_{37}^\circ / \text{kcal mol}^{-1}$
H1A/H1B 	44.7	86.2	245	10.1
I1A/I1B	49.5	93.3	265	11.2
J1A/J1B	47.0	83.6	236	10.5
K1A/K1B	41.1	79.0	226	8.8
H2A/H2B 	47.1	86.9	246	10.7
K2A/K2B	40.3	81.8	235	8.8
H6A/H6B 	61.3	102.0	279	15.4
K6A/K6B	47.4	85.4	241	10.7
P0/N ^b	47.7	89.9	254	11.2
A1A/T1B ^b	49.4	94.0	266	11.6
G1A/C1B ^b	53.4	100.5	282	13.1
A2A/T2B	49.2	101.6	289	11.9
A6A/T6B	53.6	134.2	385	14.9

^a Solution conditions: [ODN] = 5.0 μ M, [NaCl] = 100 mM, pH 7.0 (10 mM phosphate buffer) ^b Data from ref. 27.

effect of **H–H** with a conventional natural base pair.²⁷ **A1A/T1B** and **G1A/C1B** gave higher T_m s than **H1A/H1B**. Similarly, the T_m of **A2A/T2B** was higher than that of **H2A/H2B**. However, the T_m of six A–T pairs (**A6A/T6B**: 53.6 °C) was lower than that of six **H–H** pairs (**H6A/H6B**: 61.3 °C); **H–H** pairs were more stable than A–T pairs when multiple **H–H** pairs were introduced. The T_m s of other artificial base pairs are also listed in Table 1. On the other hand, artificial bases carrying aromatic moieties stabilized the duplex in spite of the incorporation of a single pair; T_m s of **I1A/I1B** and **J1A/J1B** containing a benzene ring were 49.5 and 47.0 °C, respectively, which were comparable or even higher than that of the native duplex.

The thermodynamic parameters of these duplexes determined from $1/T_m$ versus $\ln(C_T/4)$ plots are listed in Table 1. The $-\Delta G_{37}^\circ$ value of **H1A/H1B** was 10.1 kcal mol⁻¹, which was less than that of **P0/N** (11.2 kcal mol⁻¹). However, when the number of **H–H** pairs increased to two, $-\Delta G_{37}^\circ$ increased by 0.6 kcal mol⁻¹ (**H2A/H2B**). Furthermore, $-\Delta G_{37}^\circ$ of **H6A/H6B** was as high as 15.4 kcal mol⁻¹, which was 4.2 kcal mol⁻¹ higher than that of **P0/N** without artificial base pairs. In addition, the $-\Delta G_{37}^\circ$ was even 0.5 kcal mol⁻¹ larger than that of **A6A/T6B**. The larger $-\Delta G_{37}^\circ$ of **H6A/H6B** was mainly attributed to the $-\Delta S$, which was 106 cal mol⁻¹ K smaller than that of **A6A/T6B**, whereas its $-\Delta H$ was 32.2 kcal mol⁻¹ smaller. These results strongly suggested that a smaller loss in entropy due to hydrophobic interaction between **H** moieties contributed to the large T_m .

The $-\Delta G_{37}^\circ$ of the base pairs synthesized here was in the order of **I–I** (11.2 kcal mol⁻¹ \approx **P0/N**) > **J–J** (10.5) \approx **H–H** (10.1) > **K–K** (8.8), which did not necessarily coincide with the number of benzene rings in the base-surrogate. For example, the **H–H** pair with isopropylcyclohexane was almost comparable with the **J–J** pair having a biphenyl. Stability of a **K–K** pair was 1.3 kcal mol⁻¹ lower than that of an **H–H** pair. Furthermore, the difference of $-\Delta G_{37}^\circ$ between **H6A/H6B** and **K6A/K6B** was as high as 4.7 kcal mol⁻¹, demonstrating that hydrophobic interactions between

isopropyl groups contributed strongly to the stabilization of the duplex.

2.3 Shielding efficiency of cyclohexyl base pairs as insulators

Next, we applied these cyclohexyl base pairs to suppress electron transfer in DNA. Natural DNA nucleobases are known to be good mediators for hole/electron transfer.^{28–32} However, since the cyclohexyl base pair reported here has no π electrons, it should be a good “insulator” of electron transfer when it is located next to natural nucleobases. In order to evaluate the insulating ability of cyclohexyl base pairs, we investigated the fluorescence recovery of pyrene by the incorporation of cyclohexyl moieties. DNA–pyrene conjugates have been widely used as fluorescence probes and labeling agents.^{14–16,33–38} We have also introduced pyrene between natural base pairs and prepared fluorescence probes and labeling agents.^{39–41} However, quenching by nucleobases severely limits the detection sensitivity; the quantum yield of pyrene is as low as 0.003, especially when multiple pyrenes are introduced between natural base pairs.⁴¹ Since this quenching is attributable to electron transfer from pyrene to nucleobases,³³ we incorporated cyclohexyl base pairs between pyrene and nucleobases as insulators to enhance the emission of pyrene, as we previously applied to perylene diimide²⁴ (see Fig. 1). Kool *et al.* reported that 5,6-dihydro-2'-deoxythymidine, which they inserted between pyrene and thymidine, enhanced the emission of pyrene in the single-stranded state.⁴² In our study, we utilized the base pairing of cyclohexyl moieties in order to suppress the undesired dynamic quenching. Fluorescence enhancement by cyclohexyl base pairs has the potential to improve the sensitivity of pyrene-based fluorescent probes and labeling agents.

Sequences of modified DNA are shown in Fig. 1b and schematically illustrated in Fig. 1a. We incorporated two or six cyclohexyl base pairs (**H–H** and **K–K** pairs) between the pyrene and nucleobases. In addition, **I–I** and **J–J** pairs were also introduced in order to evaluate the effect of chemical structure on the insulating ability. **P1/N**, which contains no cyclohexyl base pairs, but a pyrene moiety, was synthesized as a control. **P1/N** showed almost no fluorescence, as shown in the purple line in Fig. 5, because the emission from pyrene was severely quenched by nucleobases. The quantum yield of pyrene was determined to be

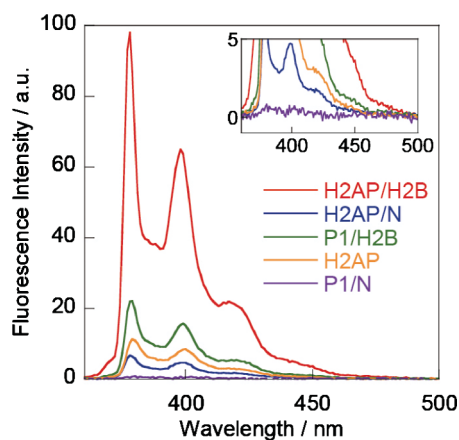


Fig. 5 Fluorescence emission spectra of **H2AP/H2B**, **H2AP/N**, **P1/H2B**, single-stranded **H2AP** and **P1/N** at 20 °C. Conditions: [NaCl] = 100 mM, pH 7.0 (10 mM phosphate buffer), [ODN] = 1.0 μ M.

Table 2 Spectroscopic behaviors and thermodynamic stabilities of the modified ODNs

Sequence	Relative Intensity ^a	ϕ^b	$\lambda_{\max}/\text{nm}^c$	$T_m/^\circ\text{C}^d$
H2AP/H2B	1	0.19	346	48.5
I2AP/I2B	0.70	— ^e	347	52.2
J2AP/J2B	<0.01	— ^e	347	52.6
K2AP/K2B	0.91	— ^e	346	43.1
P1/N	<0.01	<0.01	351	48.6
P1	0.02	— ^e	350	—
H2AP	0.16	— ^e	348	—
H2AP/N	0.07	0.02	348	43.2
P1/H2B	0.22	0.05	348	47.5
H6AP/H6B	1.71	0.32	345	62.0
I6AP/I6B	1.49	— ^e	346	63.8
K6AP/K6B	1.65	— ^e	345	49.8
H6AP	0.67	— ^e	346	—

^a Emission intensity at 378 nm relative to that of **H2AP/H2B**. Solution conditions: [ODN] = 1.0 μ M, [NaCl] = 100 mM, pH 7.0 (10 mM phosphate buffer) ^b Quantum yield determined from the quantum yield of pyrene in N_2 -bubbled cyclohexane (0.65) used as a reference. ^c Absorption maximum of pyrene in the UV-Vis spectrum at 20 °C. ^d Solution conditions: [ODN] = 5.0 μ M, [NaCl] = 100 mM, pH 7.0 (10 mM phosphate buffer) ^e Not determined.

below 0.01 (Table 2).⁴³ On the other hand, incorporation of **H–H** pairs greatly increased its emission. **H2AP/H2B**, which contains two **H–H** pairs between pyrene and the neighboring base pairs, showed intense peaks at around 380 and 400 nm (red line in Fig. 5). The quantum yield of **H2AP/H2B** increased to 0.19 (Table 2).

Consequently, the incorporation of two **H–H** pairs increased the quantum yield of pyrene by more than hundred times. In contrast, such a large enhancement of the quantum yield was not observed with single-stranded **H2AP**; the emission intensity of **H2AP** was about six times lower than that of **H2AP/H2B** (see Fig. 5 and Table 2). In addition, **H2AP/N** and **P1/H2B**, which contained two **H** moieties in one strand, showed much weaker emission than **H2AP/H2B**. Thus, the base pairing of **H** moieties is required for the large enhancement of the fluorescence intensity of pyrene.

We next evaluated the effect of the chemical structure on the shielding effect. **K–K** pairs showed an almost comparable shielding effect to that of **H–H** pairs (compare **K2AP/K2B** with **H2AP/H2B** in Fig. 6 and Table 2). Accordingly, the isopropyl group is not essential for the shielding effect, although it remarkably contributed to the stability of the duplex. Although **I2AP/I2B**, containing cyclohexylbenzene, exhibited a slightly lower emission intensity than **H2AP/H2B** (compare the blue line with the red in Fig. 6), the emission intensity was still remarkably higher than **P1/N**, showing that introduction of one benzene ring did not severely decrease the emission intensity. However, incorporation of the

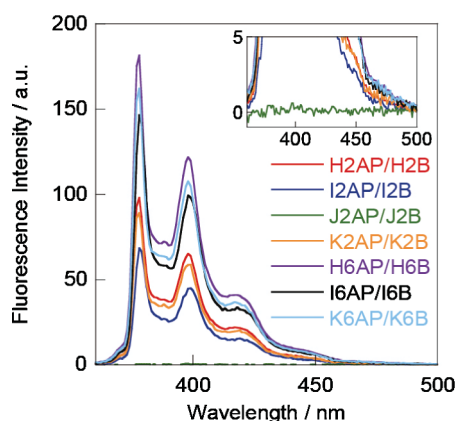


Fig. 6 Fluorescence emission spectra of **H2AP/H2B**, **I2AP/I2B**, **J2AP/J2B**, **K2AP/K2B**, **H6AP/H6B**, **I6AP/I6B**, and **K6AP/K6B** at 20 °C. Conditions: [NaCl] = 100 mM, pH 7.0 (10 mM phosphate buffer), [ODN] = 1.0 μ M.

J–J pairs with biphenyl moieties substantially lowered the emission intensity; **J2AP/J2B** emitted almost the same fluorescence as **P1/N** did. From these comparisons, we concluded that at least one cyclohexane ring is necessary in order to enhance the emission of pyrene.

Further increases in the number of cyclohexyl base pairs moderately enhanced the fluorescence. **H6AP/H6B**, which contained six **H–H** pairs between the pyrene and nucleobases, showed a 1.7-times higher emission than **H2AP/H2B** (compare the red line with the purple in Fig. 6) and its quantum yield was as high as 0.32 (Table 2). On the other hand, the emission intensity of single-stranded **H6AP** was only about one-third of that of **H6AP/H6B**. Similarly, incorporation of six **I–I** pairs or **K–K** pairs also enhanced the fluorescence intensity, although the intensity of **I6AP/I6B** was slightly lower than those of **H6AP/H6B** and **K6AP/K6B** (Fig. 6 and Table 2).

The melting temperatures of these duplexes are summarized in Table 2. The T_m s of duplexes sandwiched with two insulator pairs were in the following order: **J2AP/J2B** (52.6 °C) \approx **I2AP/I2B** (52.2 °C) > **H2AP/H2B** (48.5 °C) (\approx **P1/N**; 48.6 °C) \gg **K2AP/K2B** (43.1 °C). Similarly, **K6AP/K6B** having six **K–K** pairs showed the lowest T_m (49.8 °C), while those of **H6AP/H6B** and **I6AP/I6B** were as high as 62.0 and 63.8 °C, respectively. This is because the hydrophobic interactions of **H–H** pairs having isopropylcyclohexane also efficiently worked even when pyrene was inserted between them.

UV-Vis spectra of **H2AP/H2B**, **H6AP/H6B**, and **P1/N** are shown in Fig. 7. Both **H2AP/H2B** and **H6AP/H6B** showed a sharp band at 346 and 345 nm assignable to the pyrene moiety, respectively. On the other hand, the absorption maximum of **P1/N** was located at 351 nm, which was about 5 nm longer than that of **H2AP/H2B** or **H6AP/H6B** and was broadened. These spectral changes also support the shielding of pyrene from nucleobases (*vide infra*).

Discussion

3.1 High stability of multiple cyclohexyl base pairs

The incorporation of a single **H–H** pair slightly lowered duplex stability, although cyclohexyl moieties were located inside the

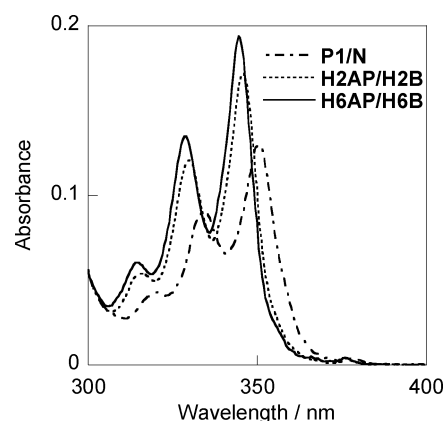


Fig. 7 UV-Vis spectra of **H2AP/H2B**, **H6AP/H6B** and **P1/N** at 20 °C. Conditions: [NaCl] = 100 mM, pH 7.0 (10 mM phosphate buffer), [ODN] = 5.0 μ M.

DNA duplex, as revealed by NMR analysis in the case of **H–K** “base pair”. Since a non-planar **H** moiety and planar natural nucleobase should cause steric hindrance, hydrophobic interactions between isopropyl groups should not compensate for the destabilization caused by the disturbance of aromatic stacking interactions between nucleobases. Consistent with this, **I1A/I1B** or **J1A/J1B**, which involve aromatic rings, have higher T_m s due to aromatic stacking interactions, as well as hydrophobic interactions.²³ However, the accumulation of non-planar **H–H** pairs did not further destabilize the duplex, but largely stabilized the duplex. In addition, $-\Delta G^\circ_{37}$ did not proportionally increase with the number of **H–H** pairs; the increase in $-\Delta G^\circ_{37}$ per **H–H** pair between **H2A/H2B** and **H6A/H6B** was 1.17 kcal mol⁻¹, while it was only 0.6 kcal mol⁻¹ between **H1A/H1B** and **H2A/H2B**. Such a steep stabilization of **H6A/H6B** is attributable to the accumulated hydrophobic interactions among the consecutive **H** moieties with less steric hindrance between them. All of the cyclohexyl moieties with chair-shaped configurations may be well accommodated in the duplex and overcompensate the destabilization induced at the boundary of **H–H** and natural base pairs. In addition, hydrophobic interactions between isopropyl groups in the **H–H** pair are also significant because **K–K** pairs with a methyl group on the cyclohexyl ring less efficiently stabilized the duplex. Taken together, we conclude that hydrophobic interactions without aromatic stacking interactions can be a strong driving force of DNA hybridization.

3.2 Insulating ability of cyclohexyl base pairs

The incorporation of an **H–H** pair between nucleobases and pyrene efficiently enhanced the emission of pyrene; the emission intensity of **H2AP/H2B** was more than hundred times higher than that of **P1/N** (see Fig. 5) because pyrene was efficiently shielded from natural nucleobases.⁴⁴ The suppressed interaction between pyrene and nucleobases was also substantiated from a comparison of the UV spectra of **H2AP/H2B** with **P1/N**, as shown in Fig. 7; both **H2AP/H2B** and **H6AP/H6B** showed a sharp band at 346 and 345 nm, respectively, whereas **P1/N** had a maximum at 351 nm with reduced absorbance (hypochromism). This difference is interpreted as follows. In **P1/N**, pyrene was intercalated between the adjacent nucleobases. Under these conditions, a

strong excitonic interaction of pyrene with nucleobases induced both bathochromicity and hypochromicity compared with isolated pyrene absorption.^{45,46} However, in the cases of **H2AP/H2B** and **H6AP/H6B**, isopropylcyclohexane moieties inserted between the pyrene and nucleobases efficiently isolated pyrene and blocked their excitonic interaction. Accordingly, the insertion of the **H-H** pair induced hypochromicity and hyperchromicity.

Among the insulators synthesized in this study, **J-J** pairs with biphenyl moieties did not show “shielding effects”, as demonstrated by **J2AP/J2B** (Fig. 6). Since the **J-J** pair did not destabilize the duplex, as shown in Table 1, it should be located inside the DNA duplex.^{47,48} Indeed, bands of pyrene in **J1AP/J1B** showed strong hypochromism compared to the other duplexes (see Fig. S2 in the Supporting Information†), but note that these spectral changes were not derived from the excitonic interaction between the nucleobase and pyrene. The intercalated biphenyl moiety that has a similar UV-Vis spectrum to the nucleobase excitonically interacted with pyrene, resulting in strong hypochromism. Since a **J** residue has two benzene rings, electron transfer from nucleobases occurred through the π electrons of the benzene rings and, thus, quenched their emission. From these results, we think that at least one cyclohexane ring is necessary for the enhancement of the quantum yield of pyrene.

The fluorescence intensity of **I2AP/I2B** was slightly lower than that of **H2AP/H2B**, although its intensity was much higher than **P1/N**. The same tendency was observed with **I6AP/I6B** and **H6AP/H6B**. It is likely that the benzene ring of the **I** moiety might slightly quench the fluorescence of pyrene. In contrast, **K-K** pairs without benzene rings showed almost the same shielding effect as **H-H** pairs, demonstrating that the isopropyl group in the **H** moiety did not contribute to the shielding. However, the absence of an isopropyl group destabilizes the duplex, which is a severe problem when multiple chromophores and insulators are introduced into DNA.⁴¹ Taken together, **H-H** pairs are the best “insulator” among the four molecules.

3.3 Effect of the number of insulators

In this study, the incorporation of a single **H-H** pair between the pyrene and nucleobases drastically increased the emission intensity. On the other hand, the introduction of two additional pairs only moderately enhanced the emission of pyrene. In the DNA duplex, electron transfer over short distances proceeds by a superexchange mechanism.^{28–32} Consequently, the rate of electron transfer should decay exponentially with the distance. Here, the cyclohexyl insulator has no aromatic rings, so it could not be involved in the electron transfer process. In our system, the difference in quantum yield between **H2AP/H2B** and **H6AP/H6B** is not large, whereas that between **P1/N** and **H2AP/H2B** is massive. This high distance-dependence might reflect exponential decay in the superexchange process. However, there are several factors that might affect the apparent recovery of pyrene emission: 1) the hydrophobic environment created by cyclohexyl base pairs might change the emission intensity of pyrene. In order to rule out this possibility, a reporter dye monitoring the hydrophobicity of the microenvironment should be introduced between the cyclohexyl base pairs; 2) The mobility of the cyclohexane rings might affect the efficiency. Note that neither **H-H** nor **K-K** pairs were associated with hydrogen bonding or electrostatic

interactions, so that together these pairs may have high mobility even in the duplex. Accordingly, fixing an “insulator pair” by incorporating associative interactions (such as hydrogen bonding) would be the next step to suppress the undesired dynamics for further development of the insulator pair.

4. Conclusion

We successfully prepared novel artificial bases that formed a pair through hydrophobic interactions. These “base pairs” of isopropylcyclohexane moieties showed even higher stability than natural A–T pairs, although the moiety had no aromatic rings or hydrogen bonds. Thermodynamic analyses demonstrated that hydrophobic interactions between isopropyl groups contributed significantly to the stability. In NOESY of duplexes containing a cyclohexyl base pair (isopropylcyclohexane-methylcyclohexane pair), distinct signals were observed between the methyl protons of cyclohexyl moieties and imino protons of both the neighboring base pairs. In addition, interhelical NOEs between cyclohexyl moieties were also observed. CD spectra showed that a duplex containing as many as six cyclohexyl base pairs still kept the native B-form duplex. These results clearly demonstrated that cyclohexyl moieties without aromatic rings formed a “base pair” inside the DNA duplex.

When the artificial base pairs were introduced between pyrene and nucleobases, cyclohexyl moieties worked as “insulators”, and the emission intensity of pyrene greatly increased. The quantum yield of a duplex containing one pair of isopropylcyclohexane was as high as 0.19, which was more than hundred times higher than the yield of a duplex without insulators. The cyclohexyl base pairs were located between pyrene and the bases and efficiently disturbed the electron transfer between them. Previously, we proposed new methodology of accumulating fluorophores into DNA duplex by mimicking quantum dots for its application to “bright” labelling of biomolecule.⁴¹ We demonstrated that a DNA-based fluorophore assembly could easily be labelled onto long DNA only by treatment with ligase. However, available dyes were limited to perylene derivatives since most of fluorophores such as Cy3 significantly lowered the quantum yield by their intercalation due to the strong quenching by natural nucleobases. If we use cyclohexyl base pairs in place of natural base-pairs, various fluorescent dyes can be accumulated without decreasing quantum yield. Such fluorophore assembly has potential as sensitive labelling agent of biomolecules to detect them at the single-molecule level.

5. Experimental

5.1 Materials

All of the conventional phosphoramidite monomers, CPG columns, reagents for DNA synthesis and Poly-Pak II cartridges were purchased from Glen Research. Other reagents for the synthesis of phosphoramidite monomers were purchased from Tokyo Kasei Co., Ltd and Aldrich.

5.2 Synthesis of the DNA modified with pyrene and insulators

All of the modified ODNs were synthesized on an automated DNA synthesizer (ABI-3400 DNA synthesizer, Applied

Biosystems) using phosphoramidite monomers bearing pyrene and insulators. Phosphoramidite monomer tethering a methylcyclohexane moiety (**K** residue) was synthesized as described in the Supporting Information†. Phosphoramidite monomers of other non-natural moieties and pyrene were prepared according to previous reports.^{24,40} The coupling efficiency of the monomers corresponding to the modified residues was as high as that of the conventional monomers, as judged from the coloration of the released trityl cation. After the recommended work-up, they were purified by reversed phase (RP)-HPLC and were characterized by MALDI-TOFMS (Autoflex, Bruker Daltonics). Purities of all the ODNs are estimated over 99% from HPLC analysis.

The MALDI-TOFMS data for the DNA were as follows:

H1A: Obsd 3962 (calcd for [**H1A** + H⁺]: 3964). **H2A**: Obsd 4283 (calcd for [**H2A** + H⁺]: 4283). **H6A**: Obsd 5558 (calcd for [**H6A** + H⁺]: 5560). **H1B**: Obsd 3962 (calcd for [**H1B** + H⁺]: 3964). **H2B**: Obsd 4281 (calcd for [**H2B** + H⁺]: 4283). **H6B**: Obsd 5559 (calcd for [**H6B** + H⁺]: 5560). **I1A**: Obsd 3999 (calcd for [**I1A** + H⁺]: 3998). **I1B**: Obsd 3999 (calcd for [**I1B** + H⁺]: 3998). **I2B**: Obsd 4351 (calcd for [**I2B** + H⁺]: 4351). **I6B**: Obsd 5764 (calcd for [**I6B** + H⁺]: 5764). **J1A**: Obsd 3992 (calcd for [**J1A** + H⁺]: 3992). **J1B**: Obsd 3992 (calcd for [**J1B** + H⁺]: 3992). **J2B**: Obsd 4341 (calcd for [**J2B** + H⁺]: 4339). **K1A**: Obsd 3936 (calcd for [**K1A** + H⁺]: 3936). **K1B**: Obsd 3937 (calcd for [**K1B** + H⁺]: 3936). **K2A**: Obsd 4225 (calcd for [**K2A** + H⁺]: 4227). **K2B**: Obsd 4227 (calcd for [**K2B** + H⁺]: 4227). **K6A**: Obsd 5391 (calcd for [**K6A** + H⁺]: 5391). **K6B**: Obsd 5393 (calcd for [**K6B** + H⁺]: 5391). **P1**: Obsd 4081 (calcd for [**P1** + H⁺]: 4082). **H1C**: Obsd 2112 (calcd for [**H1C** + H⁺]: 2112). **K1D**: Obsd 2084 (calcd for [**K1D** + H⁺]: 2084). **H2AP**: Obsd 4719 (calcd for [**H2AP** + H⁺]: 4720). **I2AP**: Obsd 4788 (calcd for [**I2AP** + H⁺]: 4788). **J2AP**: Obsd 4776 (calcd for [**J2AP** + H⁺]: 4776). **K2AP**: Obsd 4664 (calcd for [**K2AP** + H⁺]: 4664). **H6AP**: Obsd 5995 (calcd for [**H6AP** + H⁺]: 5997). **I6AP**: Obsd 6201 (calcd for [**I6AP** + H⁺]: 6201). **K6AP**: Obsd 5826 (calcd for [**K6AP** + H⁺]: 5829).

5.3 Spectroscopic measurements

Fluorescence spectra were measured on a JASCO model FP-6500 with a microcell. The excitation wavelength was 345 nm. The sample solutions were as follows: [NaCl] = 100 mM, pH 7.0 (10 mM phosphate buffer), [ODN] = 1.0 μM. Quantum yields were determined from the quantum yield of pyrene in N₂-bubbled cyclohexane (0.65) as a reference.

UV-Vis and CD spectra were measured on a Shimadzu UV-1800 and a JASCO model J-820, respectively, with a 10-mm quartz cell equipped with programmed temperature controllers. The sample solutions were as follows: [NaCl] = 100 mM, pH 7.0 (10 mM phosphate buffer), [ODN] = 5.0 μM.

5.4 Measurement of the melting temperature

The melting curve of duplex DNA was obtained with a Shimadzu UV-1800 by measurement of the change in absorbance at 260 nm versus temperature. The melting temperature (T_m) was calculated from the maximum in the first derivative of the melting curve. Both the heating and the cooling profiles were measured and its average was determined as T_m . The temperature ramp was 0.5 °C min⁻¹ and the T_m s determined from heating and cooling profiles agreed

to within 2.0 °C. The sample solutions were as follows: [NaCl] = 100 mM, pH 7.0 (10 mM phosphate buffer), [ODN] = 5.0 μM.

Thermodynamic parameters of duplexes (ΔH , ΔS) were determined from $1/T_m$ versus $\ln(C_T/4)$ plots by the following equation: $1/T_m = R/\Delta H \ln(C_T/4) + \Delta S/\Delta H$, where C_T is the total concentration of ODNs. ΔG_{37}° was calculated from the ΔH and ΔS values. The sample solutions were as follows: [NaCl] = 100 mM, pH 7.0 (10 mM phosphate buffer). The range of DNA concentrations was 2–64 μM.

5.5 NMR measurements

NMR samples were prepared by dissolving three-times lyophilized DNA in an H₂O/D₂O 9:1 solution containing 10 mM sodium phosphate (pH 7.0) to give a duplex concentration of 1.7 mM. NaCl was added to give a final sodium concentration of 200 mM.

NMR spectra were measured with a Varian INOVA spectrometer (700 MHz) equipped for triple resonance at a probe temperature of 275 K. Resonances were assigned by standard methods using a combination of 1D, TOCSY (60 ms of mixing time), DQF-COSY, and NOESY (150 ms of mixing time) experiments. All spectra in the H₂O/D₂O 9:1 solution were recorded using the 3-9-19 WATERGATE pulse sequence for water suppression.

5.6 Computer modeling

Molecular modeling by conformational energy minimization was performed with Insight II/Discover 3 software (Molecular Simulation, Inc.) on a Silicon Graphics Octane workstation with the operating system IRIX64 Release 6.5 and AMBER was used for the calculations. The results of the NMR analyses served as a starting point for the modeling (no restraints were used for energy minimization).

Acknowledgements

This work was partially supported by a Grant-in-Aid for Scientific Research (A) (21241031) and a Grant-in-Aid for Young Scientists (B) (22750149) from the Ministry of Education, Culture, Sports, Science and Technology, Japan. Partial support by SENTAN program, Japan Science and Technology Agency (JST), is also acknowledged.

Notes and references

- 1 B. A. Schweitzer and E. T. Kool, *J. Am. Chem. Soc.*, 1995, **117**, 1863–1872.
- 2 C. Brotschi, A. Häberli and C. J. Leumann, *Angew. Chem., Int. Ed.*, 2001, **40**, 3012–3014.
- 3 H. Liu, J. Gao, S. R. Lynch, Y. D. Saito, L. Maynard and E. T. Kool, *Science*, 2003, **302**, 868–871.
- 4 N. Minakawa, N. Kojima, S. Hikishima, T. Sasaki, A. Kiyosue, N. Atsumi, Y. Ueno and A. Matsuda, *J. Am. Chem. Soc.*, 2003, **125**, 9970–9982.
- 5 S. Matsuda and F. E. Romesberg, *J. Am. Chem. Soc.*, 2004, **126**, 14419–14427.
- 6 N. Amann, R. Huber and H.-A. Wagenknecht, *Angew. Chem., Int. Ed.*, 2004, **43**, 1845–1847.
- 7 Z. Yang, D. Hutter, P. Sheng, A. M. Sismour and S. A. Benner, *Nucleic Acids Res.*, 2006, **34**, 6095–6101.
- 8 I. Hirao, T. Mitsui, M. Kimoto and S. Yokoyama, *J. Am. Chem. Soc.*, 2007, **129**, 15549–15555.
- 9 S. Hainke and O. Seitz, *Angew. Chem., Int. Ed.*, 2009, **48**, 8250–8253.

- 10 F. D. Lewis, T. Wu, E. L. Burch, D. M. Bassani, J.-S. Yang, S. Schneider, W. Jaeger and R. L. Letsinger, *J. Am. Chem. Soc.*, 1995, **117**, 8785–8792.
- 11 F. D. Lewis, Y. Zhang and R. L. Letsinger, *J. Am. Chem. Soc.*, 1997, **119**, 5451–5452.
- 12 S. M. Langenegger and R. Häner, *Helv. Chim. Acta*, 2002, **85**, 3414–3421.
- 13 U. B. Christensen and E. B. Pedersen, *Helv. Chim. Acta*, 2003, **86**, 2090–2097.
- 14 U. B. Christensen and E. B. Pedersen, *Nucleic Acids Res.*, 2002, **30**, 4918–4925.
- 15 S. M. Langenegger and R. Häner, *Chem. Commun.*, 2004, 2792–2793.
- 16 P. J. Hrdlicka, B. R. Babu, M. D. Sorensen, N. Harrit and J. Wengel, *J. Am. Chem. Soc.*, 2005, **127**, 13293–13299.
- 17 R. Häner, F. Garo, D. Wenger and V. L. Malinovskii, *J. Am. Chem. Soc.*, 2010, **132**, 7466–7471.
- 18 S. A. Benner, *Acc. Chem. Res.*, 2004, **37**, 784–797.
- 19 K. Tanaka and M. Shionoya, *Chem. Lett.*, 2006, **35**, 694–699.
- 20 A. T. Krueger and E. T. Kool, *Curr. Opin. Chem. Biol.*, 2007, **11**, 588–594.
- 21 J. Štambaský, M. Hocek and P. Kočovský, *Chem. Rev.*, 2009, **109**, 6729–6764.
- 22 V. L. Malinovskii, D. Wenger and R. Häner, *Chem. Soc. Rev.*, 2010, **39**, 410–422.
- 23 M. Kaufmann, M. Gisler and C. J. Leumann, *Angew. Chem., Int. Ed.*, 2009, **48**, 3810–3813.
- 24 H. Kashida, K. Sekiguchi and H. Asanuma, *Chem.–Eur. J.*, 2010, **16**, 11554–11557.
- 25 H. Kashida, X. G. Liang and H. Asanuma, *Curr. Org. Chem.*, 2009, **13**, 1065–1084.
- 26 M. Liu, X.-A. Mao, C. Ye, H. Huang, J. K. Nicholson and J. C. Lindon, *J. Magn. Reson.*, 1998, **132**, 125–129.
- 27 H. Kashida, H. Ito, T. Fujii, T. Hayashi and H. Asanuma, *J. Am. Chem. Soc.*, 2009, **131**, 9928–9930.
- 28 G. B. Schuster, *Acc. Chem. Res.*, 2000, **33**, 253–260.
- 29 F. D. Lewis, R. L. Letsinger and M. R. Wasielewski, *Acc. Chem. Res.*, 2000, **34**, 159–170.
- 30 B. Giese, *Annu. Rev. Biochem.*, 2002, **71**, 51–70.
- 31 H.-A. Wagenknecht, *Nat. Prod. Rep.*, 2006, **23**, 973–1006.
- 32 J. C. Genereux and J. K. Barton, *Chem. Rev.*, 2010, **110**, 1642–1662.
- 33 M. Manoharan, K. L. Tivel, M. Zhao, K. Nafisi and T. L. Netzel, *J. Phys. Chem.*, 1995, **99**, 17461–17472.
- 34 P. L. Paris, J. M. Langenhan and E. T. Kool, *Nucleic Acids Res.*, 1998, **26**, 3789–3793.
- 35 K. Yamana, T. Iwai, Y. Ohtani, S. Sato, M. Nakamura and H. Nakano, *Bioconjugate Chem.*, 2002, **13**, 1266–1273.
- 36 K. Fujimoto, H. Shimizu and M. Inouye, *J. Org. Chem.*, 2004, **69**, 3271–3275.
- 37 A. Okamoto, K. Kanatani and I. Saito, *J. Am. Chem. Soc.*, 2004, **126**, 4820–4827.
- 38 M. Raunkjær, K. F. Haselmann and J. Wengel, *J. Carbohydr. Chem.*, 2005, **24**, 475–502.
- 39 H. Kashida, H. Asanuma and M. Komiyama, *Chem. Commun.*, 2006, 2768–2770.
- 40 H. Kashida, T. Takatsu, K. Sekiguchi and H. Asanuma, *Chem.–Eur. J.*, 2010, **16**, 2479–2486.
- 41 H. Kashida, K. Sekiguchi, X. Liang and H. Asanuma, *J. Am. Chem. Soc.*, 2010, **132**, 6223–6230.
- 42 J. N. Wilson, Y. Cho, S. Tan, A. Cuppoletti and E. T. Kool, *ChemBioChem*, 2008, **9**, 279–285.
- 43 This quantum yield is lower than pyrene-modified DNA in other reports. In this study, 1-pyrenebutyric acid unit was introduced into DNA through D-threosinol. Accordingly, pyrene is intercalated between base pairs and is highly quenched by nucleobases. See refs 35 and 38.
- 44 We could not calculate the increasing rate of emission intensity of **H2AP/H2B** directly because the emission intensity of **P1/N** was much lower than that of **H2AP/H2B**. The emission of **P1/H2B** at high sensitivity was about 36 times higher than that of **P1/N**. In addition, the emission intensity of **H2AP/H2B** at medium sensitivity was about 4.5 times higher than that of **P1/H2B**. See Fig. S3 in the Supporting Information† for actual data.
- 45 A. Mahara, R. Iwase, T. Sakamoto, T. Yamaoka, K. Yamana and A. Murakami, *Bioorg. Med. Chem.*, 2003, **11**, 2783–2790.
- 46 A. Okamoto, K. Kanatani, Y. Ochi, Y. Saito and I. Saito, *Tetrahedron Lett.*, 2004, **45**, 6059–6062.
- 47 Z. Johar, A. Zahn, C. J. Leumann and B. Jaun, *Chem.–Eur. J.*, 2008, **14**, 1080–1086.
- 48 A. Zahn and C. J. Leumann, *Chem.–Eur. J.*, 2008, **14**, 1087–1094.